




Intensity patterns at the peaks of brain activity in fMRI and PET are highly correlated with neural models of spatial integration

Amirouche Sadoun^{1,2}  | Tushar Chauhan^{1,2} | Yi Fan Zhang^{1,2}  |
Yohan Gallois³ | Mathieu Marx³ | Olivier Deguine^{1,2,3} | Pascal Barone^{1,2} |
Kuzma Strelnikov^{1,2,3} 

¹UMR 5549, Centre National de la Recherche Scientifique, Université de Toulouse 3, Toulouse, France

²Centre de Recherche Cerveau et Cognition, Université de Toulouse 3, Université Paul Sabatier, Toulouse, France

³Service d'Oto-Rhino-Laryngologie et Oto-Neurologie, CHU de Toulouse, Université de Toulouse 3, Toulouse, France

Correspondence

Kuzma Strelnikov and Amirouche Sadoun, Cerveau & Cognition (CNRS UMR 5549), Pavillon Baudot, CHU Purpan, BP 25202, 31052 Toulouse Cedex 03 France.

Email: strelkuz@hotmail.com; am.sadoun@yahoo.fr

Abstract

Spatial integration during the brain's cognitive activity prompts changes in energy used by different neuroglial populations. Nevertheless, the organisation of such integration in 3D -brain activity remains undescribed from a quantitative standpoint. In response, we applied a cross-correlation between brain activity and integrative models, which yielded a deeper understanding of information integration in functional brain mapping. We analysed four datasets obtained via fundamentally different neuroimaging techniques (functional magnetic resonance imaging [fMRI] and positron emission tomography [PET]) and found that models of spatial integration with an increasing input to each step of integration were significantly more correlated with brain activity than models with a constant input to each step of integration. In addition, marking the voxels with the maximal correlation, we found exceptionally high intersubject consistency with the initial brain activity at the peaks. Our method demonstrated for the first time that the network of peaks of brain activity is organised strictly according to the models of spatial integration independent of neuroimaging techniques. The highest correlation with models integrating an increasing at each step input suggests that brain activity reflects a network of integrative processes where the results of integration in some neuroglial populations serve as an input to other neuroglial populations.

KEYWORDS

activity patterns, information integration, information-energy coupling, integrative models

Abbreviations: ATP, adenosine triphosphate; BOLD, blood-oxygen-level-dependent; BCa, bias-corrected and accelerated percentile algorithm for confidence intervals; CI, confidence interval; fMRI, functional magnetic resonance imaging; fNIRS, functional near-infrared spectroscopy; HbO, oxyhemoglobin; HbR, deoxyhemoglobin; NIFTI, neuroimaging informatics technology initiative; PET, positron emission tomography; SPECT, single-photon emission computerised tomography; SPM, statistical parametric mapping.

This is an open access article under the terms of the Creative Commons Attribution-NonCommercial-NoDerivs License, which permits use and distribution in any medium, provided the original work is properly cited, the use is non-commercial and no modifications or adaptations are made.

© 2021 The Authors. *European Journal of Neuroscience* published by Federation of European Neuroscience Societies and John Wiley & Sons Ltd.

1 | INTRODUCTION

In recent decades, functional neuroimaging techniques—blood-oxygen-level-dependent (BOLD) imaging in functional magnetic resonance imaging (fMRI), oxyhemoglobin (HbO) and deoxyhemoglobin (HbR) imaging in functional near-infrared spectroscopy (fNIRS) and regional cerebral blood flow and energy metabolism imaging in positron emission tomography (PET) and single-photon emission computerised tomography (SPECT)—have focused on measuring brain function related to the brain's consumption of energy. All of those approaches assume that brain activity reflects energy turnover levels in the brain and relates to information processing (Aubert et al., 2007; Shulman et al., 2004). In earlier work, we defined the term *activation* as the information-driven reorganisation of energy flows in and among populations of neuroglial units that prompt a total increase of energy use in those populations (Strelnikov, 2010). Neurons and glia (astrocytes) are tightly coupled for energy turnover and cognitive functions (Santello et al., 2019), forming functional units (Giaume et al., 2010). In that definition, *energy flows* refer to coherent spatial and temporal changes in the energy turnover of neuroglial units accompanying stimulus treatment (Strelnikov, 2010). From this point of view, it is quite natural that information about interactions between sensory molecular structures and the external world is further transmitted within the brain as neuroglial molecular interactions and causes measurable energy changes in neuroglial populations. Brain activation can be understood as the energy level in an ensemble of neuroglial units, a level, which can be reflected by different methods (e.g., BOLD fMRI and ^{15}O -water PET) (Raichle & Gusnard, 2002; Shulman et al., 2007). However, studies on the connection between energy levels in neuroglial populations and the models of information propagation have been few.

In our recent theoretical exploration (Strelnikov, 2014; Strelnikov & Barone, 2012), we suggested that tight coupling occurs between the amount of perceived information and brain energy during integrative cognitive processes. In our approach, we aim to explore the link between brain energy and information contained in cognitive stimulation. Our definition of information is that of entropy, in which energy is needed to reduce entropy in the brain, that is, to reduce uncertainty (Shannon, 1948). According to our hypothesis, information in sensory input is coded by interactions between molecular structures, which require an increase of energy input to these molecular structures. Accordingly, there is more energy turnover in neurons and astrocytes with each more integrative stage of processing, which

combines information on stimulus properties from previous stages of stimulus processing. Biochemical studies have demonstrated that one bit of information costs 10^4 adenosine triphosphate (ATP) molecules at a chemical synapse and up to 10^9 ATP molecules for spike coding (Laughlin et al., 1998; Lennie, 2003). Considering the total amount of energy at each integrative stage of sensory processing, the difference in energy levels between the stages should correspond to the difference in the amount of information coded by neuroglial populations at those stages. For example, the coupling between energy turnover and information integration was recently demonstrated for fMRI activity, which showed an amplification of local changes from low-level acoustic cortical regions to high-level cortical regions that accumulate and integrate information (Yeshurun et al., 2017).

It has been demonstrated that the propagation of information in the brain tends to follow the direction of activity gradients (spatial increments between adjacent voxels) with significant divergences of gradients in the sensory cortices and convergences in the brain's integrative centres (Strelnikov & Barone, 2012). In that context, the propagation of cortical activity in the direction of its spatial gradients has been attributed to large-scale travelling waves (Roberts et al., 2019), as confirmed in studies on electric field dynamics in the cortex (e.g., (Alekseichuk et al., 2019)). Likewise, optogenetic investigations have suggested that perceptually relevant information is pooled across functionally confined local cortical populations and that such pooled information is further transmitted to more integrative areas (Andrei et al., 2019).

While some studies indicate that there is an increase in brain activity related to the integration of stimulus properties, these studies use the term “integration” in the purely descriptive sense suggesting on the ground of cognitive reasoning that there is an accumulation of information processed between cortical sites. None of the studies explored whether the sites of information integration can be detected in the brain according to the integration model, in which each voxel integrates information from other voxels. The principle of energy optimisation demonstrated by the above discussed studies suggests that energy turnover in the brain should closely match information processing needs. This has led us to the idea that using cross-correlation, one can detect voxels in the brain, in which energy turnover closely matches the modelled integrative functions as suggested by integrative neural models (Kuzma, 2019; Strelnikov, 2014).

To combine the mentioned experimental and theoretical evidence of the propagation of information in the direction of increased brain activity, in our study, we sought the possibility to detect integrative patterns of

brain activity in neuroimaging data. To that end, we used an integrative model corresponding to approximately the same amount of information received by each neural node and transmitted to the next one (Figure 1a). Another tested option was the linearly increasing input to each voxel (Figure 1b). The model depicted in Figure 1 (Kuzma, 2019; Strelnikov, 2014) served as the initial theoretical guess for the choice of integrative functions. For the non-linear modelled input, we chose non-trivial zeros of the Riemann zeta function because they are associated with energy levels at the atomic level (Schumayer & Hutchinson, 2011) (Bogomolny, 2007) and cannot be expressed as an arithmetic combination of linear functions. If supported, our hypothesis would explain the observed increase of the modelled information content in the direction of activity increase (i.e., in the direction of activity gradients) because more energy is needed for a greater amount of information en route to being integrated.

2 | MATERIALS AND METHODS

2.1 | Datasets

We used data from two fMRI studies, one of which is publicly accessible, along with data from two PET activation studies using $H_2^{15}O$. Contrast images reflect the average difference between the stimulation and baseline

condition (they are not the same as t-maps). In addition, to verify the robustness of the analysis, we created random images of brain activity (“Random dataset”) using a uniform distribution. For the first dataset, referred to as “WH2015,” freely available data were chosen from the study of Wakeman and Henson (Wakeman & Henson, 2015) conducted with 16 participants (ftp://ftp.mrc-cbu.cam.ac.uk/personal/rik.henson/wakemandg_hensonrn/). The MATLAB scripts attached to the original dataset were used for preprocessing and statistical analysis using the MATLAB SPM toolbox, which resulted in contrast images in the MNI space with 3-mm isotropic voxels. In the original study, the subjects were presented with grayscale images of familiar and unfamiliar faces, as well as faces scrambled by a 2D Fourier transform, all of which were cropped using a mask based on a combination of the familiar and unfamiliar faces. We used the contrast “Faces (familiar + unfamiliar) > scrambled” for the analysis.

The second fMRI dataset, called “fMRI auditory,” was for auditory processing and originated from our research on speech processing conducted with 15 participants (Strelnikov, Rouger, Belin, et al., 2011; Strelnikov & Barone, 2012). Participants lay in the scanner with eyes closed and listened to 13 disyllabic words, one of which was randomly repeated, and the participants were instructed to press the button when they heard the repeated word. The dataset comprised the contrasts “Words > silent baseline” per subject.

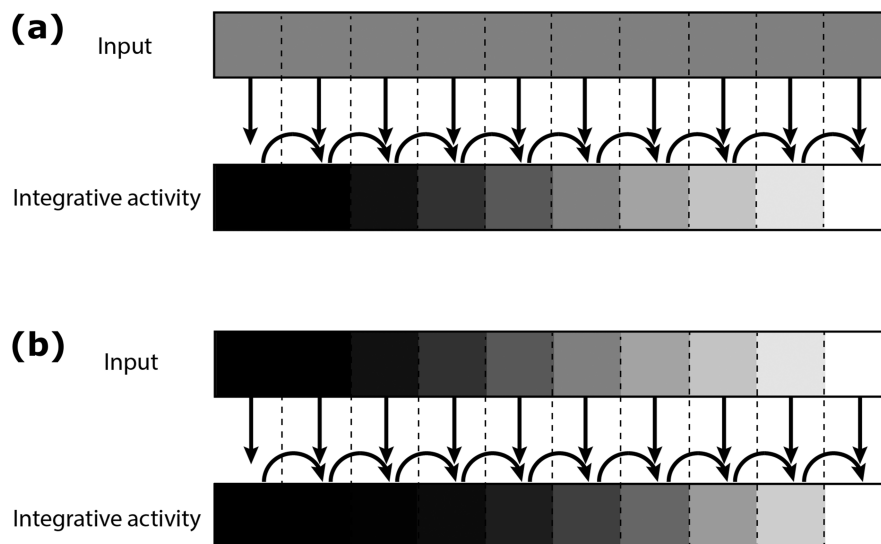


FIGURE 1 Presumable schemes of information integration by a series of voxels. (a) After each voxel (node of the model) in the array receives the same quantity of information, the voxels transmit the information among each other, thereby increasing brain activity, which corresponds to the increase in the amount of treated information. (b) The input to each voxel is already the result of integration (i.e., ‘integrative activity’ in (a)), and as the voxels transmit information from left to right, they prompt the increase of their activity, which corresponds to the further integration of information. For other graphical representations and explanations of the integrative functions used in our analysis, see Figure S1 in supporting information

In the first PET study, we used our dataset about word perception, dubbed “PET S2011,” with five participants (Strelnikov, Rouger, Eter, et al., 2011). The reference condition was purely visual and consisted in recognising visually presented signs (i.e., either “+” or “×”) that appeared one by one in a randomised order on the screen. Each participant was instructed to click the PC’s mouse: one button for “+” and another for “×”. During the auditory condition, words and non-words were presented binaurally, such that each participant had to identify whether he heard a word or a non-word. We analysed the contrasts between the word/non-word identification and the baseline.

For the second PET dataset, called “PET S2015,” we used our data on audiovisual word processing with six participants (Strelnikov et al., 2015). During the baseline condition, participants lay in the scanner with their eyes closed and without any auditory stimulation. The audiovisual speech condition involved presenting videos with sound, and we asked participants to identify words by using a computer mouse (two-alternative forced choice). We analysed the contrasts between audiovisual stimulation and the baseline.

2.2 | Data analysis

To model integrative activity (Figure 1), we used the vectors of 100 values. Activity with the constant input (Figure 1a) was modelled with the function $g(t) = t$, in which t runs from 1 to 100. Afterwards, to obtain the vectors of 100 integrated values from the linear and zeta non-trivial zero values as inputs, we applied the following integral function:

$$I(x) = \int_0^x g(t) dt$$

Riemann’s zeta values for non-trivial zeros (imaginary parts) were obtained using the zeta zero function in the Python package `mpmath`. (See Figure 2 for the flow-chart of the further analysis.)

Contrast images of brain activity were transformed to NIfTI format using `MRICron` and imported using the Python package `NiBabel`. Next, 3D images were vectorised in ascending order while preserving the initial position indices, and intensities were normalised between 0 and 255. One percent of the smallest values was discarded as artefacts of the non-neural origin.

Both vectors (i.e., the probe and the one obtained from the 3D image) were normalised considering the mean and standard deviation. Thereafter, the vector obtained from the 3D image was cross-correlated with

the probe vectors of 100 values to obtain the position of maximum correlation (i.e., cross-correlation with Fourier transform). At this position, the Pearson correlation coefficient was calculated.

Next, we calculated spatial overlap between the voxels issued from cross-correlation and the peaks of activity in the initial images. Voxels from the image vector at the highest correlation site were marked by adding 255 to the initial normalised values, after which the initial 3D position was restored. Thus, we obtained 100 marked voxels in the 3D space of the initial contrast images. The resulting image was saved in neuroimaging informatics technology initiative (NIfTI) format.

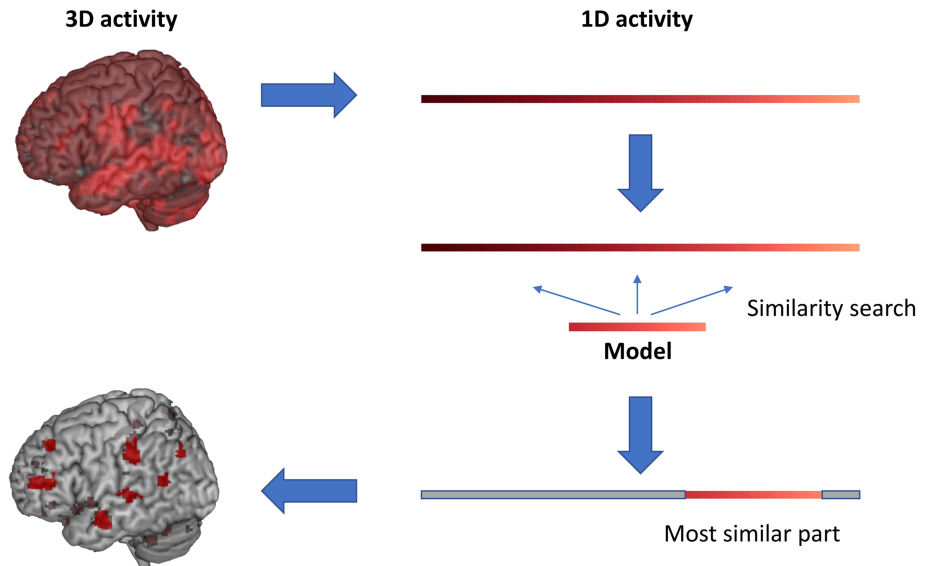
To calculate spatial overlap of the restored images with the initial images of brain activity, the initial images were thresholded using the value at which the maximum correlation with the model occurred. Images issued from the cross-correlation were thresholded so as to preserve only the marked voxels (i.e., with the threshold of 255). After that, the initial and restored thresholded images were binarised and multiplied. After the multiplication, the sum of non-zero voxels served to calculate the percentage of spatial overlap between the images issued from cross-correlation and the peaks of activity in the initial images.

The significance of correlation coefficients for different models and functions was assessed using bootstrapping with bias-corrected and -accelerated (BCa) percentile algorithm for confidence intervals (i.e., resampled 10,000 times with a BCa percentile algorithm for confidence intervals; Carpenter & Bithell, 2000). Paired bootstrapping was also performed to compare correlation coefficients using Bonferroni correction for the number of comparisons. Furthermore, in an additional analysis, given the small number of subjects in both PET datasets (due to the invasive nature of PET), we combined them into one set of 11 subjects (i.e., five subjects of the PET S2011 dataset and six of the second) in order to perform the same bootstrapping analysis because increasing the sample size increased the statistical power.

Next, we calculated the derivatives and the derivatives of the natural logarithm of the brain activity for all the datasets to check if the slopes of the vectors were similar or different between the subjects’ brain activities.

Lastly, we performed another analysis using three randomised probe vectors to check for possible random effects on cross-correlations. The first one contained 100 permuted values taken from the 100 highest values in the vectorised 3D images; the second was taken from the middle of the vectorised 3D images, and the third was built from a uniform distribution in the range of the image intensities. Those vectors were cross-correlated with the vectorised activity obtained from the 3D image.

FIGURE 2 The flowchart of the analysis. The 3D activity was transformed into the 1D array. Afterwards, we searched for the fragments of activity, which are the most similar to the modelled ones, using cross-correlation as a measure of similarity. Having found the most similar to the model fragment of the 1D array, we restored the 3D positions of these voxels



3 | RESULTS

Data analysis revealed an important difference between the integrative model with a spatially constant input and the integrative models with the spatially increasing input. After the cross-correlation analysis of probe vectors with one-dimensional brain activity, we restored voxels' spatial positions at the loci of the maximum cross-correlation. We found that those positions spatially overlapped with peaks of activity in the initial images.

In the following, we describe the results obtained using the fMRI and PET datasets.

3.1 | fMRI data

The analysis of the fMRI datasets showed a significantly higher correlation for the integrative models with the increasing input (linear and non-linear increase) compared with the constant input model, as indicated by the absence of overlap between the constant input model's 95% bootstrapped confidence interval (CI) and the CI of the models with increasing input ($p < 0.05$, paired bootstrap; Figure 3a,b and Table 1). Correlations for the model with linear input were significant and higher than for the model with non-linear input ($p < 0.05$, paired bootstrap; see supporting information for the correlation coefficients per image and supporting information Figures S1 and S2).

Those results indicate that the integrative models with increasing input are more representative than the integrative models with the constant input with respect to brain activity in our analysis of the BOLD signal in the "stimulation versus baseline" contrast maps.

3.2 | PET data

We found that the integrative models with the increasing input in the PET S2011 and combined PET datasets have a significantly higher correlation than the integrative model with the constant input (Figure 4 and Table 1; $p < 0.05$, paired bootstrap). However, no significant differences were found between the correlations with the linear and non-linear inputs in the PET S2011 dataset, possibly due to the sample's insufficient size (see supporting information for the correlation coefficients per image).

In the PET S2015 dataset, the integrative models with the increasing input have also significantly higher correlation than the constant input one (Figure 4, Table 1). The linear increasing input model's correlations were slightly but significantly superior to the non-linear input model in the PET S2015 dataset and the combined two datasets ($p < 0.05$, paired bootstrap; see supporting information for the correlation coefficients per image).

Thus, separate and combined results on PET datasets are in line with results on fMRI datasets and indicate that the integrative models with the increasing input are more representative than the integrative constant input models with respect to the brain activity as reflected by the regional cerebral blood flow in "stimulation versus baseline" contrast maps.

In all of the fMRI and PET datasets, we compared the distribution of brain activity in contrast images with normal distribution and found that it differed significantly from normal in each image (D'Agostino–Pearson test for moderate and large samples, $p < 0.001$).

We also tested the model fit using PCA and R^2 estimations, which confirmed that models with the increasing linear and non-linear inputs had a better fit

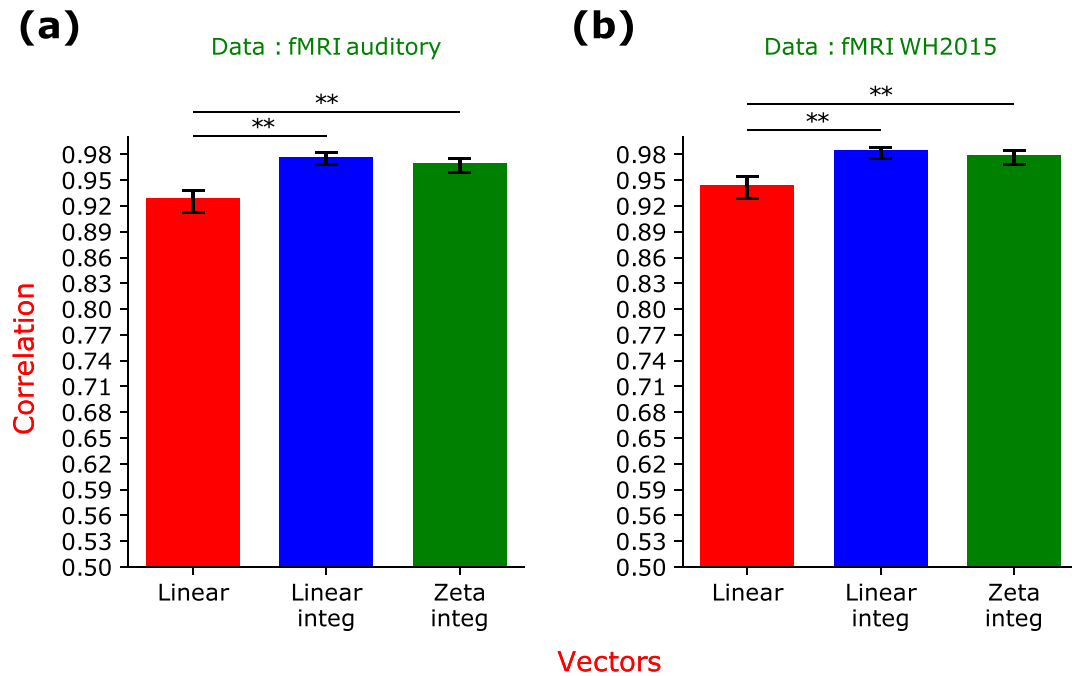


FIGURE 3 Results of the correlations obtained for each model in the fMRI datasets. Panels (a) and (b) display results of the correlations for each dataset and for each model: Linear = linear model (i.e., with the constant input). Linear integ = linear integrated model. Zeta integ = model with integrated Riemann's zetas' non-trivial zeros (i.e., models with the increasing input). Error bars represent 95% bootstrapped confidence intervals of correlation values (resampling 10,000 times with a bias-corrected and accelerated percentile algorithm for confidence intervals (Carpenter & Bithell, 2000)). These are **unpaired** bootstrap confidence intervals, which test the significance of each correlation with respect to zero, depicted here for illustrative purposes. Paired bootstrap was used to estimate the differences between the models (which are reported in the results section). ** = significant

TABLE 1 Summary of correlation results, with mean values and 95% bootstrapped confidence intervals (CI) indicated for each probe vector and dataset

Datasets		Mean			Bootstrapped CI [inf, sup]		
		Linear	Linear_integ	Zeta_integ	Linear	Linear_integ	Zeta_integ
fMRI	fMRI auditory	0,928	0,976	0,968	[0,912, 0,936]	[0,968, 0,981]	[0,958, 0,974]
	fMRI WH2015	0,943	0,984	0,978	[0,928, 0,954]	[0,974, 0,988]	[0,967, 0,984]
PET	PET images S2011	0,946	0,983	0,978	[0,919, 0,977]	[0,978, 0,990]	[0,967, 0,989]
	PET images S2015	0,937	0,978	0,972	[0,885, 0,960]	[0,953, 0,988]	[0,940, 0,986]
	PET images S2011 and S2015	0,941	0,980	0,975	[0,913, 0,960]	[0,966, 0,986]	[0,957, 0,984]

Note: These are unpaired bootstrap confidence intervals, which test the significance of each correlation with respect to zero. Paired bootstrap was used to estimate the differences between the models (see Section 3).

Abbreviations: fMRI, functional magnetic resonance imaging; PET, positron emission tomography.

than the model with the constant input (see supporting information).

3.3 | Random dataset

Cross-correlation analysis of random brain activity resulted in random locations, far from the maximum values and variable for different integrative models precluding the comparison between their correlation values. Correlations with random probe vectors were extremely

low (see supporting information Figure S3). These results indicate that random effects cannot explain the reported correlations in fMRI and PET datasets.

3.4 | Spatial overlap

We calculated the percentage of spatial overlap between the voxels resulting from the cross-correlation and the peaks of activity in the initial contrast maps. The analysis revealed an overlap of 99% (Figure 5) for all datasets and

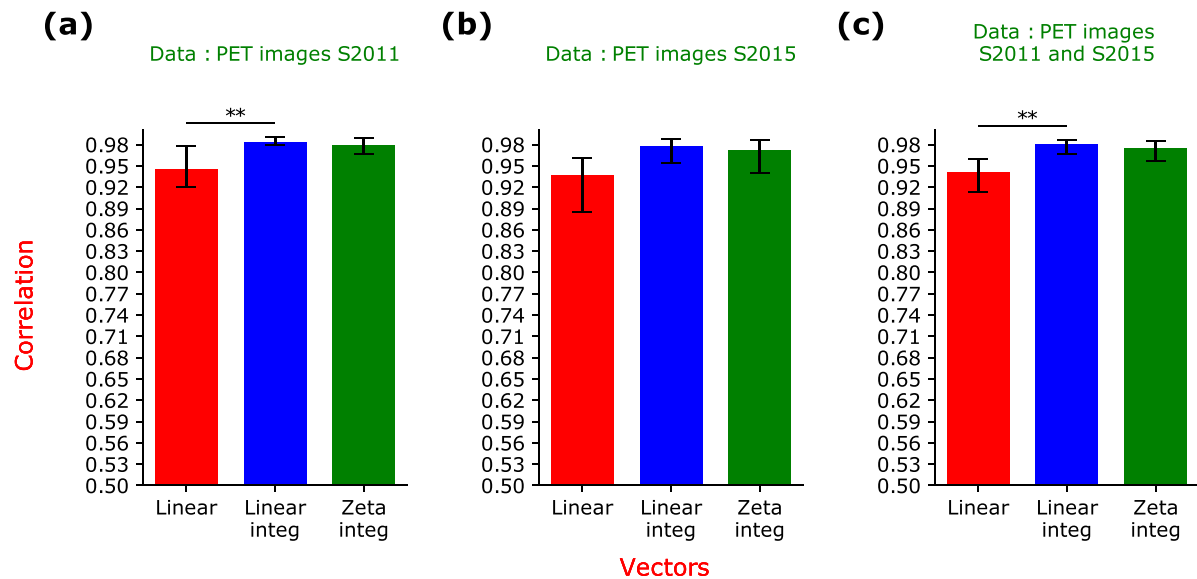


FIGURE 4 Results of the correlations obtained for each model concerning the PET datasets. Panels (a), (b) and (c) display the results of the correlations for each dataset and each model. Panel c demonstrates the confidence intervals (CI) for the combined datasets (i.e., S2011 + S2015). Linear = linear model model (i.e., with the constant input). Linear integ = linear integrated model. Zeta integ = model with integrated Riemann's zetas' non-trivial zeros (i.e., models with the increasing input). Error bars represent the 95% bootstrapped CIs of correlation values, resampled 10,000 times with a bias-corrected and -accelerated percentile algorithm for CIs (Carpenter & Bithell, 2000). These are **unpaired** bootstrap confidence intervals, which test the significance of each correlation with respect to zero, depicted here for illustrative purposes. Paired bootstrap was used to estimate the differences between the models (which are reported in the results section). ** = significant

all subjects except the 16th one in the 1st fMRI dataset (WH2015), who had 93.39% spatial overlap. For that subject, the number of voxels at the peak of activity was 106 and larger than the probe vector's size, which contained only 100 values. That surprisingly robust result indicates that all of the voxels corresponding to the highest correlation values with integrative models were situated within the peaks of brain activity as reflected by contrast maps during cognitive loads.

The result with 99% spatial overlap is valid for all types of integrative models in our analysis. In turn, it follows that integrative processing occurs at peaks of brain activity.

Given the results of control analyses on random datasets, our cross-correlation results on real datasets indicate that (a) the highest correlations for integrative models are very consistently found at the peaks of activity and (b) they are higher for the integrative models with the increasing input compared with the constant input integrative model.

4 | DISCUSSION

We examined the integrative patterns in brain activity originating from stimulus-specific contrasts provided by

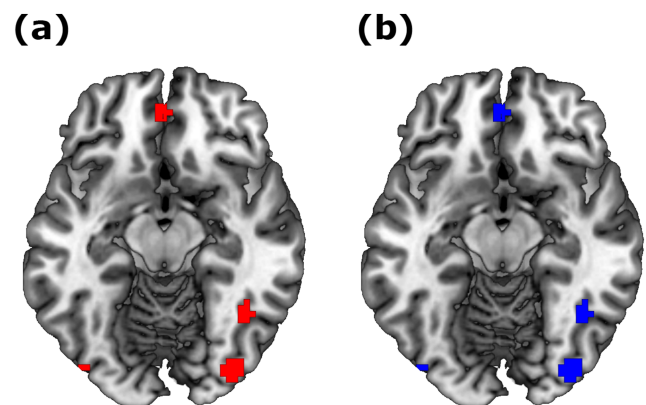


FIGURE 5 Example of initial thresholded image and image of voxels issued from maximal cross-correlation with integrative models. In the initial image (a), activity peaks were present in the occipital and orbitofrontal cortex. The same localisations were detected using cross-correlation with all types of integrative models (b). The example is for subject 5, WH2015 dataset

fMRI and PET neuroimaging techniques. According to our hypothesis, brain activity contains sequences of voxels that integrate inputs to these voxels (Figure 1). To test that theoretically driven hypothesis, we constructed probe vectors with mathematical models of the two possibilities of integration:

1. with the same quantity of information received per voxel (Figure 1a)
2. with increasing input of information received per voxel (Figure 1b)

For the second type of mathematical model, we tested both the linear and non-linear increase of the input; the chosen non-linear function corresponded to Riemann's non-trivial zeros. Correlations aimed to compare, which theoretical predictions are a better match for brain activity, the constant input to the voxels or the linearly increasing input.

The constant input corresponds to the linear function, and the linear/non-linear input corresponds to the integral of the linear/non-linear function (Figure 1). We obtained high correlations with both types of models, and both models pointed to the same set of voxels, which were the most active ones. Having restored those voxels' spatial location, we found that they corresponded exactly to the spatial peaks of brain activity. Although correlations were strong for the model with the constant input, they were significantly higher—up to 0.99 for some subjects—for the probe vector modelling the integration of the increasing input to voxels. That finding implies that integrative models with spatially increasing input can more precisely describe between-voxel activity at peak levels. Within the peaks of activity, the treatment of sensory stimuli is likely to be organised according to the integration of their properties. According to our results, the input to each voxel at peaks of activity was already the result of the integration of information from less active voxels (Figure 1b). Transmitting the information between the voxels as shown in Figure 1 seems to increase the activity, which corresponds to the further integration of information.

Furthermore, we found the same pattern of information integration at all peaks of activity during the presentation of complex stimuli (i.e., faces and words). Because processing complex stimuli requires different functions (e.g., processing colour, shape, and edges in the visual domain), the existence of such patterns of integration may support the hypothesis that stimuli features are not processed at the same time; information about each feature needs to be integrated on the basis of the previously integrated information. Another probable hypothesis is that information about several stimuli features may arrive at higher-activity areas at the same time, and in that case, such information might be integrated with previously memorised information. Both of those mechanisms may exist in the brain and contribute to the observed integrative activity.

In one of the PET datasets (PET S2011) no significant differences were found between the correlations with the

linear and non-linear inputs, possibly due to the sample's insufficient size. In all datasets, the highest correlation values were observed at the loci of the one-dimensional brain activity with the highest slopes (See supporting information Figures S4 to S8). In that context, a higher slope indicates a higher difference between voxels, meaning that voxels at peaks of activity have the highest differences in activity between the adjacent voxels (i.e., spatial gradients). The transfer of integrated information along the gradient vectors of brain activity has been shown with fMRI data (Strelnikov & Barone, 2012) and later explained by the large-scale propagation of travelling waves (Roberts et al., 2019).

Thus, our method permitted us to reliably identify peaks of brain activity using integrative models with spatially increasing inputs. Being aware of the possible technical and data-processing issues that can result in correlations, we applied our method to the data of different fMRI and PET machines using different subjects and different types of stimulation, and we obtained the same results concerning the correlations of integrative models of brain activity within peaks of activity.

With all of those datasets, contrasts were created using MATLAB SPM software. By extension, following a supporting explorative approach, we investigated a set of random, unprocessed 3D images obtained using different fMRI and PET scanners, including ones from our laboratory, and found that all of them followed the same rule as reported here for contrasts, with correlations of up to 0.99 at peaks of activity in the case of integrative functions, albeit in different regions. Thus, the correlations obtained with integrative models exist even in the unprocessed raw data, though they correspond to different loci than in the contrasts images, and these correlations did not result from the treatment of images performed to obtain stimulation-specific contrasts. At the same time, they were specific neither to a particular scanner nor to a particular brain-imaging technique. Therefore, our results provide evidence that peaks of activity in "stimulation vs. baseline" contrasts correspond to loci where spatial integration in stimulus-induced activity exceeded that in the baseline activity.

Nevertheless, even having examined various sources of technical artefacts, we cannot definitely reject their absence. Such uncertainty follows from the logic that although it is possible to prove the existence of a phenomenon (e.g., a certain artefact), it is impossible to prove its absence. Even in the case that some unknown technical artefacts generate the highest correlations with integrative probe vectors at peaks of activity, the methodological value of our results remains intact because the existence of those correlations was proven with high certainty with various datasets and neuroimaging

techniques. To our knowledge, no such method of peak detection is described in the literature on neuroimaging.

With the mentioned precautions in mind, we can return to our neurophysiological and neuroenergetic hypotheses that spurred our investigation. The average level of metabolic activity (i.e., metabolic energy) in a voxel, which can be indirectly measured by fMRI and PET, indicates the level of interaction between different molecules. In turn, that level approximately corresponds to the internal energy of the voxel or the free energy according to the thermodynamic interpretation of the free energy theory (Friston & Stephan, 2007). If the level of energy is higher in the given voxel, at least from a purely mechanical perspective, then a spread of energy from that voxel to the adjacent ones can be expected, similarly to air moving in space from locations with high pressure to locations with lower pressure. Ultimately, the result would be the decrease of the differences in energy between adjacent voxels during stimulation. However, we have shown the existence of stimulation-specific spatial differences (i.e., gradients) between the adjacent voxels (Strelnikov & Barone, 2012). We suggested that some general forces are related to information processing, which maintain the observed local differences (i.e., gradients) of activity. Our present results go further and suggest that persistent stimulation-specific differences are the highest between the voxels at the peaks of brain activity and can be considered as a sequence of integrative activity. Although that observation does not follow the free-energy minimisation principle at the local scale, it does not contradict the principle at the global scale of the brain–environment interaction.

In quantum physics, the Montgomery–Odlyzko conjecture (Odlyzko, 1987) states that the distribution of spaces between successive non-trivial zeros of a suitably normalised Riemann zeta function is statistically identical to the distribution of eigenspaces in the Gaussian unitary ensemble (a mathematical model used to describe energy levels in quantum mechanics). Although Riemann's non-trivial zeros could be a better predictor than a linear function for metabolic energy, our study revealed that the correlation of brain activity with the integral of the linear function is slightly but significantly higher than for Riemann's non-trivial zeros. That result could be attributed to both technical and theoretical reasons. The technical reason is that PET and fMRI do not measure metabolic energy directly but provide an indirect measure related to blood flow and oxygenation, which may blur the subtle quantum effects. The theoretical explanation, by contrast, may rest in the fact that the Gaussian unitary ensemble describes isolated quantum phenomena, which are not implicated in information processing. The brain may be a unique organ that couples

information with quantum energy so that information processing may impose specific laws of energy transformation in complex molecular systems. Both explanations can contribute to the overall linear integrative effect observed in our study.

From a physiological point of view, however, the constant increase of energy turnover due to the integration of a large amount of information may prompt energy levels beyond the capacity of glucose and oxygen supply to neuroglial populations. To cope with that problem, a mechanism of energy-based feedback may exist, in which rescaling activity constantly occurs but does not influence the spatial coding of information (Kuzma, 2019). The necessity of downscaling energy expenditure can explain a large network of feedback mechanisms, all of which rescale energy-related differences between the stages of information integration to match the physiological capacities of energy turnover. Such energy-saving downscaling allows the brain activity to maintain the representation of stimuli-related information in spatially organised patterns of brain activity (Sadoun et al., 2020). The advantage of that mechanism is that coding can be maintained not by energy levels per se but by the spatial differences in energy that can be adjusted according to updated stimulations from the environment and neuronal feedback.

Our study has demonstrated that brain activity peaks contain voxels, which follow the models of integration almost exactly. The question of what happens in voxels outside the peaks of activity remains, however. Although they should also accumulate information and transmit it to other voxels, smaller amounts of information may be processed with lower amounts of energy, which are nearly within the limits provided by normal blood flow and oxygenation. Thus, our integrative models may not apply to other voxels simply because relatively low metabolic processes in other voxels do not sufficiently change blood flow and oxygenation, which underlie PET and fMRI signals. When amounts of treated information require significant additional energy input from extracerebral sources, the integrative law of energy consumption becomes evident with the techniques, which measure events outside neuroglial tissue. Given those assumptions, our findings do not reject integrative models of information–energy coupling for the entire brain but nevertheless confirm integrative models in neuroglial populations with the highest activity.

5 | CONCLUSIONS

In several fMRI and PET datasets, the statistical comparison confirmed the higher match for integrative models, in which the input increases at each step of integration

between the nodes of the model. In this way, we provide the first evidence that one can computationally detect sites, which closely follow the law of spatial integration in the brain. Interestingly, the correlated with integrative models sites are situated at the peaks of activity in the fMRI and PET data. These findings suggest that the network of brain activity at its peaks is spatially organised according to models of information integration.

ACKNOWLEDGEMENTS

The authors are very grateful to Daniel Wakeman and Richard Henson for data availability, data citation: Wakeman, D. G. & Henson, R. N. *OpenfMRI ds000117* (2014).

CONFLICT OF INTEREST

The authors declare no conflicts of interests.

ETHIC STATEMENT

WH2015 dataset: As precised in Wakeman and Henson's study, their study "was approved by Cambridge University Psychological Ethics Committee. Written informed consent was obtained from each participant prior to and following each phase of the experiment. Participants also gave separate written consent for their anonymised data to be freely available on the internet.". Likewise, they mentioned that "All research was conducted in accordance with the Declaration of Helsinki (1964)" (Wakeman & Henson, 2015).

fMRI auditory dataset: as mentioned by Strelnikov, Rouger, Belin, et al. (2011), their work has been "approved by the local research ethics committee of Glasgow University". In addition, "All of the subjects gave their full and informed consent prior to their participation in accordance with the Declaration of Helsinki (1968)." (Strelnikov, Rouger, Belin, et al., 2011).

PET 2011 dataset: as indicated by Strelnikov, Rouger, Eter, et al. (2011), their study has been approved by the local ethical committee: "The study was approved by the local ethical committee (CCPPRB-Toulouse 1: dossier no. 1-06-13)". In addition, "all subjects signed a written informed consent in accordance with the Declaration of Helsinki (1968)." (Strelnikov, Rouger, Eter, et al., 2011).

PET 2015 dataset: as indicated by Strelnikov et al. (2015), their work has been approved by the local ethical committee, and "all participants gave their fully informed consent prior to their inclusion in this study, in accordance with local ethics committees (CPRB Toulouse I, no. 1-04-47, Toulouse, France)". Likewise, "the study conformed to the 2013 WMA Declaration of Helsinki." (Strelnikov et al., 2015).

AUTHOR CONTRIBUTIONS

AS: study design, scripts and programming conception, methodology development, data analysis, statistical analysis, results discussion and interpretation and manuscript preparation. T C: manuscript preparation, statistical models verification and discussion, data analysis and data analysis verification and results discussion and interpretation. YZ: manuscript draft preparation, data analysis verification and results discussion and interpretation. YG: manuscript draft preparation, data analysis verification and results discussion and interpretation. MM: manuscript draft preparation and results discussion and interpretation. OD: experiments conception and design, manuscript draft preparation and results discussion and interpretation. PB: experiments conception and design, manuscript draft preparation and results discussion and interpretation. KS: study design, experiments conception and design, performed the experiments, methodology development, scripts and programming conception, data analysis verification, results discussion and interpretation, manuscript preparation and project supervision. All authors reviewed the manuscript and discussed the results.


PEER REVIEW

The peer review history for this article is available at <https://publons.com/publon/10.1111/ejn.15469>.


DATA AVAILABILITY STATEMENT

Data generated and analysed in this study as well as the scripts are available online (https://osf.io/sywkm/?view_only=50bcf54a986348739a273e482e023331).

ORCID

Amirouche Sadoun  <https://orcid.org/0000-0003-0606-8738>

Yi Fan Zhang  <https://orcid.org/0000-0002-9688-6867>

Kuzma Strelnikov  <https://orcid.org/0000-0002-6613-2300>

REFERENCES

- Alekseichuk, I., Falchier, A. Y., Linn, G., Xu, T., Milham, M. P., Schroeder, C. E., & Opitz, A. (2019). Electric field dynamics in the brain during multi-electrode transcranial electric stimulation. *Nature Communications*, *10*(1), 2573. <https://doi.org/10.1038/s41467-019-10581-7>
- Andrei, A. R., Pojoga, S., Janz, R., & Dragoi, V. (2019). Integration of cortical population signals for visual perception. *Nature Communications*, *10*(1), 3832. <https://doi.org/10.1038/s41467-019-11736-2>
- Aubert, A., Pellerin, L., Magistretti, P. J., & Costalat, R. (2007). A coherent neurobiological framework for functional neuroimaging provided by a model integrating compartmentalized

- energy metabolism. *Proceedings of the National Academy of Sciences of the United States of America*, 104(10), 4188–4193. <https://doi.org/10.1073/pnas.0605864104>
- Bogomolny, E. (2007). Riemann zeta function and quantum chaos. *Progress of Theoretical Physics Supplement*, 166, 19–36. <https://doi.org/10.1143/PTPS.166.19>
- Carpenter, J., & Bithell, J. (2000). Bootstrap confidence intervals: When, which, what? A practical guide for medical statisticians. *Statistics in Medicine*, 19(9), 1141–1164. [https://doi.org/10.1002/\(SICI\)1097-0258\(20000515\)19:9<1141::AID-SIM479>3.0.CO;2-F](https://doi.org/10.1002/(SICI)1097-0258(20000515)19:9<1141::AID-SIM479>3.0.CO;2-F)
- Friston, K. J., & Stephan, K. E. (2007). Free-energy and the brain. *Synthese*, 159(3), 417–458. <https://doi.org/10.1007/s11229-007-9237-y>
- Giaume, C., Koulakoff, A., Roux, L., Holcman, D., & Rouach, N. (2010). Astroglial networks: A step further in neuroglial and gliovascular interactions. *Nature Reviews Neuroscience*, 11(2), 87–99. <https://doi.org/10.1038/nrn2757>
- Kuzma, S. (2019). Energy-information coupling during integrative cognitive processes. *Journal of Theoretical Biology*, 469, 180–186. <https://doi.org/10.1016/j.jtbi.2019.03.005>
- Laughlin, S. B., De Ruyter van Steveninck, R. R., & Anderson, J. C. (1998). The metabolic cost of neural information. *Nature Neuroscience*, 1(1), 36–41. <https://doi.org/10.1038/236>
- Lennie, P. (2003). The cost of cortical computation. *Current Biology*, 13(6), 493–497. [https://doi.org/10.1016/S0960-9822\(03\)00135-0](https://doi.org/10.1016/S0960-9822(03)00135-0)
- Odlyzko, A. M. (1987). On the distribution of spacings between zeros of the zeta function. *Mathematics of Computation*, 48(177), 273–308. <https://doi.org/10.1090/S0025-5718-1987-0866115-0>
- Raichle, M. E., & Gusnard, D. A. (2002). Appraising the brain's energy budget. *Proceedings of the National Academy of Sciences of the United States of America*, 99(16), 10237–10239. <https://doi.org/10.1073/pnas.172399499>
- Roberts, J. A., Gollo, L. L., Abeyesuriya, R. G., Roberts, G., Mitchell, P. B., Woolrich, M. W., & Breakspear, M. (2019). Metastable brain waves. *Nature Communications*, 10(1), 1056. <https://doi.org/10.1038/s41467-019-08999-0>
- Sadoun, A., Chauhan, T., Mameri, S., Zhang, Y. F., Barone, P., Deguine, O., & Strelnikov, K. (2020). Stimulus-specific information is represented as local activity patterns across the brain. *NeuroImage*, 223, 117326. <https://doi.org/10.1016/j.neuroimage.2020.117326>
- Santello, M., Toni, N., & Volterra, A. (2019). Astrocyte function from information processing to cognition and cognitive impairment. *Nature Neuroscience*, 22(2), 154–166. <https://doi.org/10.1038/s41593-018-0325-8>
- Schumayer, D., & Hutchinson, D. (2011). Physics of the Riemann hypothesis. *Reviews of Modern Physics - REV MOD PHYS*, 83, 307–330. <https://doi.org/10.1103/RevModPhys.83.307>
- Shannon, C. E. (1948). A mathematical theory of communication. *Bell System Technical Journal*, 27(3), 379–423. <https://doi.org/10.1002/j.1538-7305.1948.tb01338.x>
- Shulman, R. G., Rothman, D. L., Behar, K. L., & Hyder, F. (2004). Energetic basis of brain activity: Implications for neuroimaging. *Trends in Neurosciences*, 27(8), 489–495. <https://doi.org/10.1016/j.tins.2004.06.005>
- Shulman, R. G., Rothman, D. L., & Hyder, F. (2007). A BOLD search for baseline. *NeuroImage*, 36(2), 277–281. <https://doi.org/10.1016/j.neuroimage.2006.11.035>
- Strelnikov, K. (2010). Neuroimaging and neuroenergetics: Brain activations as information-driven reorganization of energy flows. *Brain and Cognition*, 72(3), 449–456. <https://doi.org/10.1016/j.bandc.2009.12.008>
- Strelnikov, K. (2014). Integrative activity of neural networks may code virtual spaces with internal representations. *Neuroscience Letters*, 581, 80–84. <https://doi.org/10.1016/j.neulet.2014.08.029>
- Strelnikov, K., & Barone, P. (2012). Stable modality-specific activity flows as reflected by the neuroenergetic approach to the fMRI weighted maps. *PLoS ONE*, 7(3), e33462. <https://doi.org/10.1371/journal.pone.0033462>
- Strelnikov, K., Rouger, J., Belin, P., & Barone, P. (2011). Effects of vocoding and intelligibility on the cerebral response to speech. *BMC Neuroscience*, 12(1), 122. <https://doi.org/10.1186/1471-2202-12-122>
- Strelnikov, K., Rouger, J., Eter, E., Lagleyre, S., Fraysse, B., Demonet, J.-F., Barone, P., & Deguine, O. (2011). Binaural stimulation through cochlear implants in postlingual deafness: A positron emission tomographic study of word recognition. *Otology & Neurotology*, 32(8), 1210–1217. <https://doi.org/10.1097/MAO.0b013e31822e5bd6>
- Strelnikov, K., Rouger, J., Lagleyre, S., Fraysse, B., Demonet, J. F., Deguine, O., & Barone, P. (2015). Increased audiovisual integration in cochlear-implanted deaf patients: Independent components analysis of longitudinal positron emission tomography data. *The European Journal of Neuroscience*, 41(5), 677–685. <https://doi.org/10.1111/ejn.12827>
- Wakeman, D. G., & Henson, R. N. (2015). A multi-subject, multi-modal human neuroimaging dataset. *Scientific Data*, 2, 150001. <https://doi.org/10.1038/sdata.2015.1>
- Yeshurun, Y., Nguyen, M., & Hasson, U. (2017). Amplification of local changes along the timescale processing hierarchy. *Proceedings of the National Academy of Sciences*, 114(35), 9475–9480. <https://doi.org/10.1073/pnas.1701652114>

SUPPORTING INFORMATION

Additional supporting information may be found in the online version of the article at the publisher's website.

How to cite this article: Sadoun, A., Chauhan, T., Zhang, Y. F., Gallois, Y., Marx, M., Deguine, O., Barone, P., & Strelnikov, K. (2021). Intensity patterns at the peaks of brain activity in fMRI and PET are highly correlated with neural models of spatial integration. *European Journal of Neuroscience*, 54(9), 7141–7151. <https://doi.org/10.1111/ejn.15469>